

## Dynamically relevant structural properties of short-range spin glasses and disordered ferromagnets

G. A. Nemnes and K. H. Hoffmann

*Institut für Physik, Technische Universität Chemnitz, D-09107 Chemnitz, Germany*

(Received 29 February 2008; revised manuscript received 24 April 2008; published 22 May 2008)

Structural properties relevant for the low-temperature dynamics of short-range Ising systems are comparatively analyzed for spin glasses and disordered ferromagnets. The key elements, disorder and frustration, induce different topologies in the state space, going from funnel-like landscapes in the case of disordered ferromagnets to trapping landscapes for spin glasses. An efficient tool, dynamically relevant sequence, is introduced, which directly extracts the low-temperature dynamics.

DOI: [10.1103/PhysRevB.77.172410](https://doi.org/10.1103/PhysRevB.77.172410)

PACS number(s): 75.50.Lk

During the past years, disordered Ising spin systems such as spin glasses (SGs) and disordered ferromagnets (DFs) have become prototypical for many, rather different, fields of research. Among these are, for instance, the relaxation of ultrafast cooled atomic clusters,<sup>1</sup> the protein folding problem,<sup>2</sup> and learning and adaptation in neural networks,<sup>3</sup> as well as the evolution of financial markets.<sup>4</sup> Key features, such as *disorder* and *frustration*, present in such complex systems provide the typical roughness in the potential energy landscape<sup>5</sup> of the state space. Its structure governs the dynamical properties, ranging from highly focusing landscapes (e.g., proteins) to antifocusing (e.g., spin glasses) with respect to reaching the ground state.

Recently, the similarity between the protein folding problem and the relaxation of a disordered ferromagnet has been established.<sup>6,7</sup> Proteins are alike systems with low levels of frustration, having funnel-like potential energy landscapes,<sup>8,9</sup> which allows them to perform the biological function of folding in rather short times. In the view of Ising spin systems, this process can be regarded as a low-temperature relaxation toward the ground state, i.e., here, the dynamics concerns global kinetic properties.

The features of low-temperature spin glass dynamics are reflected in several aging experiments:<sup>10–12</sup> upon rapid cooling below the glass transition temperature, the system remains far from equilibrium on long experimental time scales. Similar behavior is exhibited by disorder ferromagnets,<sup>13–15</sup> although the observed relaxation is faster than in the spin glass case. Furthermore, some theoretical ferromagnetic models<sup>16</sup> even claim the existence of a glass transition.

This Brief Report presents a comparative study of the structural properties for both spin glass and disordered ferromagnet systems, which are relevant for describing low-temperature dynamics. Among the most important tools that have been used to quantitatively determine the dynamics of many complex systems, such as atomic clusters, proteins, or Ising spin systems for which no analytical solution is known, are kinetic Monte Carlo simulations, matrix multiplication techniques, or the graph transformation approach<sup>17</sup> to extract the mean first passage time, which are much more efficient for large systems than direct diagonalization of the transition matrix. On the other hand, the Monte Carlo Metropolis (MCM) approach becomes highly inefficient at very low temperatures. Although some improvements have been done

in the past in the form of *dynamical* (i.e., temperature dependent) Monte Carlo algorithms,<sup>18</sup> here we make use of structural properties in order to *directly* extract the low-temperature dynamics. The analysis is restricted to the smallest barriers only (i.e., saddle points), which have the major influence on the dynamics, as it will be shown in the following. This has the advantage that the time-consuming task of sampling the state space is performed once and then the results for different low temperatures are obtained with negligible effort.

The system consists of an  $N$ -dimensional hypercubic Ising lattice with short-range interactions and periodic boundary conditions. The Hamiltonian of the system is given by

$$\mathcal{H} = - \sum_{\langle i,j \rangle} J_{ij} s_i s_j, \quad (1)$$

where the sum is to be performed over all pairs of neighboring spins  $s$ , which can have only the values  $+1$  or  $-1$ . The distribution of interaction constants  $\mathcal{P}(J_{ij})$  is uniform, with zero mean and standard deviation equal to one in the case of a spin glass, resulting in the maximum interaction value  $J_{\max} = \sqrt{3}$  and  $\text{supp}(\mathcal{P}) = (-\sqrt{3}, \sqrt{3})$ . For the disordered ferromagnet, we take again a uniform distribution with the support  $(0, J_{\max})$ .

The state spaces of both SG and DF systems are collections of all possible configurations of spins (states), leading to the cardinality of  $2^{N_s}$ , where  $N_s$  is the number of spins. One defines a certain neighborhood relation (move class) as follows: two states are neighbors if they differ by one spin flip only. Thus, the state space takes the form of an  $N_s$ -regular graph (hypercube).

Typically, such landscapes contain a great number of local minima. In these discrete state spaces, a local minimum is a state which has all neighboring states with higher energy. Going from one local minimum to another using the move class indicated above, one has to pass through states of higher energies. Among all possible paths  $\mathcal{P}_{ij}$ , the one that has the smallest increase in energy provides the *saddle point* or *barrier state* between the two local minima  $i$  and  $j$ , which is the state with the highest energy in that particular path, i.e., its energy is given by

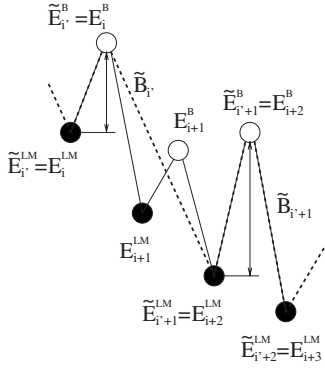


FIG. 1. Schematic of a monotonic sequence (thin line). The local minima and barrier states are represented by filled and empty circles, respectively. The dashed line indicates the DRS.

$$E_{ij}^B = \min_{\mathcal{P}_{ij}} \max_{k \in \mathcal{P}_{ij}} E_k, \quad (2)$$

where  $k$  is the state index in a path  $\mathcal{P}_{ij}$ .

In order to extract the low-temperature dynamics from the state space topology, we collect monotonic sequences<sup>19</sup> (MSs), which are characterized by the set of decreasing local minima energies  $\{E_i^{\text{LM}}\}$  and barrier state energies  $\{E_i^{\text{B}}\}$ , where  $i$  defines the step index in the sequence. They are obtained in an exact manner using a *landscape flooding* algorithm: water pours from the current escaping a local minimum and a portion of the landscape is flooded (i.e., neighboring states become submerged on a minimum energy basis) until a lower local minimum is found. In a second step, we define a *dynamically relevant sequence* (DRS) from the original MS, which is given by the new sets  $\{\tilde{E}_{i'}^{\text{LM}}\}$  and  $\{\tilde{E}_{i'}^{\text{B}}\}$ : starting with the first local minimum and barrier state after the quench, we set  $\tilde{E}_{i'=0}^{\text{LM}} = E_{i=0}^{\text{LM}}$  and  $\tilde{E}_{i'=0}^{\text{B}} = E_{i=0}^{\text{B}}$ ; then, we increment the index  $i'$  and set  $\tilde{E}_{i'}^{\text{LM}} = E_i^{\text{LM}}$  and  $\tilde{E}_{i'}^{\text{B}} = E_i^{\text{B}}$  whenever the current barrier in MS,  $B_i = E_i^{\text{B}} - E_i^{\text{LM}}$ , exceeds the current barrier in the DRS,  $\tilde{B}_{i'} = \tilde{E}_{i'}^{\text{B}} - \tilde{E}_{i'}^{\text{LM}}$ . This is schematically described in Fig. 1, where we assumed  $B_{i+1} < B_i$  and  $B_{i+2} > B_i$ . The sequence has dynamical relevance, being able to accurately reproduce the low-temperature Metropolis dynamics, which is taken as reference: all moves are trialed with equal probability and then accepted with the Metropolis probability  $P_{mn} = \min\{1, \exp[-(E_m - E_n)/T]\}$ , where  $n$  is the current state and  $m$  is the attempted neighbor.

The system preparation is typical for analyzing slow-relaxation phenomena: initially at high temperature ( $T \rightarrow \infty$ ), it is quenched in zero-temperature limit. In a first step, a rather rapid relaxation occurs, the system following a downward path toward a local minimum. In this model, it corresponds to a random state being chosen, then a random neighboring state with lower energy is selected ( $T=0$ ) until a local minimum is reached. Then, fixing a certain low but finite temperature, a phase of slow relaxation occurs, the system successively escaping from local minima into lower ones. The DRS method gives the time scales for the energy relaxation using the Arrhenius law,  $\tau_{i'} \sim \exp(\tilde{B}_{i'}/T)$ , as the system progresses toward the ground state. This construction intro-

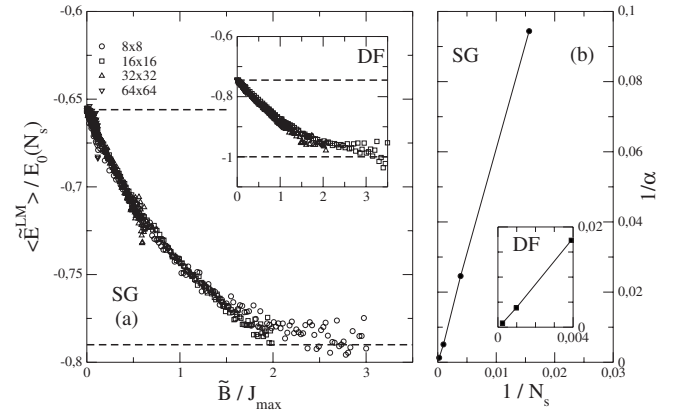


FIG. 2. (a) Average local minima energy vs monotonic barrier for different sample sizes:  $8 \times 8$  (circles),  $16 \times 16$  (squares),  $32 \times 32$  (triangles up), and  $64 \times 64$  (triangles down). The symbols for higher sample sizes overlap and cannot be clearly distinguished. The inset contains the DF case, starting with the sample size of  $16 \times 16$ . (b) Scaling of the decaying slope  $\alpha$  for the sample sizes considered.

duces the *monotonic barrier sequence*  $\{\tilde{B}_{i'}\}$ , which eliminates the smaller barriers (*skipped* barriers) that follow a larger one, since the time scales to overcome them are much shorter and the system travels to lower energies in the largest time scale so far, until an even higher barrier is reached.

More specifically, we relate the time scale  $\tau$  to overcome a barrier  $\tilde{B}$  in the DRS by

$$\tau(\tilde{B}) \approx 2\tau_0 \exp(\tilde{B}/T), \quad (3)$$

where  $\tau_0$  is the microscopic time scale for one spin flip. The factor 2 accounts for removing the barrier states in the transition matrix, which would lead to a twice as fast relaxation in the low-temperature limit, compared to the reference Metropolis dynamics.

We collect monotonic sequences of local minima for different sample sizes for both systems, SG and DF, for the two-dimensional case ( $N=2$ ), since it is computationally less expensive. Samples for the case  $N=3$  were also computed and the key features remain valid as well. In order to account for interaction randomness, we have taken 1024, 256, 64, and 16 realizations for the considered sizes of  $8 \times 8$ ,  $16 \times 16$ ,  $32 \times 32$ , and  $64 \times 64$  spins, respectively. For each sample size, ten monotonic sequences are determined within the limit of  $10^7$  states to reach a lower local minimum from the current one.

Following the rapid quench, both systems are trapped in local minima. Their energy distribution in the infinite system limit, scaled with  $E_0(N_s) = J_{\text{max}} N_s$ , is concentrating around the values of  $-0.656$  and  $-0.745$  for SG and DF, respectively. By applying a *branch and cut* algorithm,<sup>20</sup> the ground states for the SG system are exactly determined for different system sizes, resulting in an average value of  $-0.79$ . For the DF case, the infinite volume ground state is obviously  $-1.0$ .

Figure 2(a) depicts the local minima energy averaged over disorder, which was reached by crossing a certain monotonic barrier for the SG system in comparison to the DF case (in-

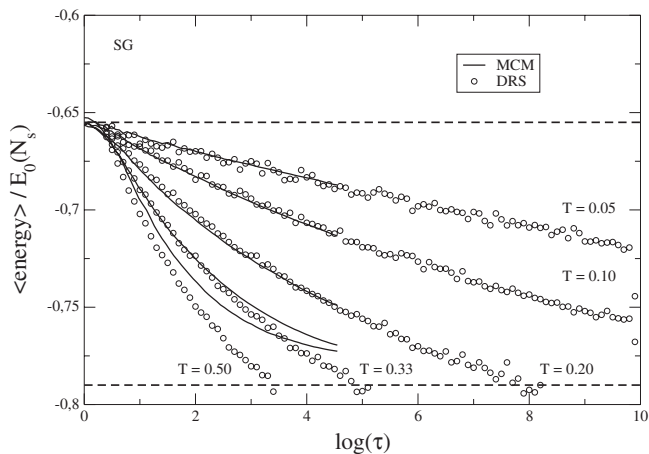


FIG. 3. Relaxation of mean energy vs time for  $16 \times 16$  SG realizations for different low temperatures: comparison between DRS (circles) and Monte Carlo Metropolis (solid lines).

set). It basically gives the time dependence of the mean energy in the slow-relaxation process for low temperatures, if one relates the time scale  $\tau$  on the monotonic barrier  $\tilde{B}$ . The data show a simple scaling of the mean energy with the number of spins  $N_s$  at least up to a time scale, giving the possibility to extrapolate the dynamical behavior of the infinite volume system in both cases. In a first order approximation, we take  $\langle \tilde{E} \rangle = e_1 E_0(N_s) - \alpha \langle \tilde{B} \rangle$ , where  $e_1 = -0.656, -0.745$  and  $\langle \tilde{E} \rangle \geq -0.75, -0.90$  for SGs and DFs, respectively. The decaying slope  $\alpha$  almost linearly increases with the system size and the average values  $\langle \alpha \rangle / E_0(N_s)$  are approximately 0.10 (SG) and 0.15 (DF) [Fig. 2(b)]. This rather good scaling behavior is a consequence of the fact that the two-dimensional Ising systems analyzed here are short-range systems.

In order to establish the accuracy of the method at low temperatures, we have compared the results obtained with DRS against the reference MCM procedure. Figure 3 shows the mean energy of  $16 \times 16$  SG systems, averaged over disorder, against the logarithm of time. The starting point after the quench, i.e., the first local minimum in each monotonic sequence or Monte Carlo run, respectively, is the same for both procedures. In the MCM approach, each spin is selected at random and flipped with the Metropolis acceptance probability, while the time is given by  $\tau = \tau_0 N_{\text{steps}}^{\text{MC}} / N_s$ , where  $N_{\text{steps}}^{\text{MC}}$  is the number of Monte Carlo steps. For the microscopic time scale, we set  $\tau_0 = 1$ . Good accuracies are achieved for temperatures up to  $T \approx 0.3$ .

To show the structural differences between the two systems, SG and DF, we have plotted in Fig. 4 three quantities (averaged over disorder) that present a high degree of correlation against the escaping local minimum energy: *barriers*, *hamming distances* ( $d^H$ ), and *number of states* ( $N_{\text{states}}$ ) visited in order to reach the barrier state from a certain escape of a local minimum. The rather comparable magnitude of the barriers [Fig. 4(a)] in both systems is due to the identical value for the maximum interaction  $J_{\text{max}}$  and a similar disorder introduced by the interaction distribution function. Qualitatively, one can observe a decrease in the average barrier for

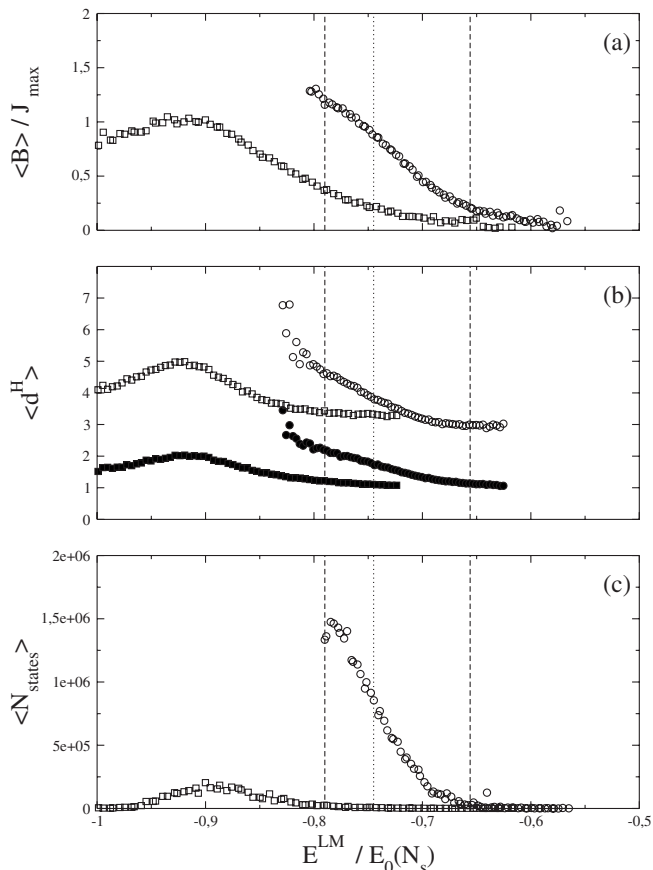


FIG. 4. Three structural quantities for SGs (circles) and DFs (squares) for a sample size of  $16 \times 16$ : (a) barriers; (b) hamming distance between the escaping local minimum and barrier state (filled), next lower local minimum (empty); (c) number of states to reach the barrier state.

DF as the system goes beyond a certain energy, which is different in the SG case. Moreover, the rate of reaching the ground state is about 82% for DFs, while for SGs, it is under 1% and in this latter case, not all of the highest barriers are found. Also, an important feature in the state space topology of both systems is the statistical increase in barrier heights with lowering the mean energy. This is not a pure dynamical effect due to our construction but indeed a structural property of the state space of the considered short-range Ising systems. The ratio of skipped barriers in the DRS is less than 25% for the sample size of  $16 \times 16$  for the SG case. This feature was also observed in other systems<sup>19</sup> and is consistent with spin glass experiments as well, in particular, aging phenomena.<sup>13</sup> Here, it is found that the system becomes *stiffer* as the age grows, i.e., the relaxation becomes slower with time and, at the same time, with decreasing energy. A similar behavior can also be observed in Figs. 4(b) and 4(c): the lower the escaping local minimum energy, the higher the hamming distances and the number of states associated with the escaping local minimum for the *frustrated* SG system, while DFs indicate a more focusing energy landscape. From the sizable structural difference in the number of states associated with the escaping local minimum, it follows that for a low but finite temperature, the escaping time into a lower

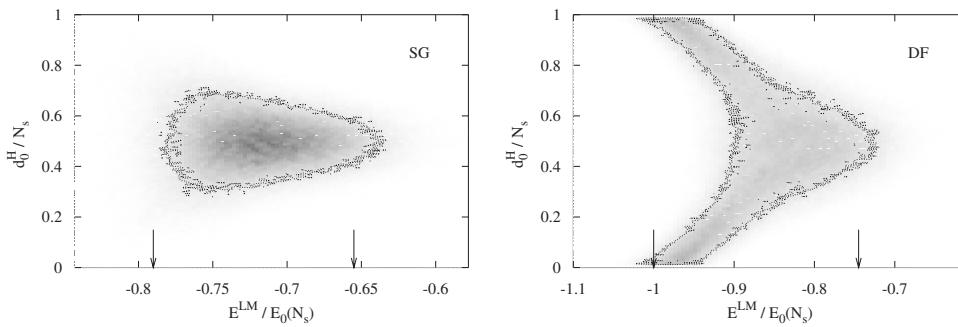


FIG. 5. Hamming distances relative to the ground state. The shaded areas represent trajectories in the  $(d_0^H, E^{LM})$  space. A relevant contour for each case was added for better visualization. The arrows mark the relaxation range for the infinite systems.

local minimum is considerably larger, the precise value depending also on the temperature and the distribution of states inside a valley.

It is well known that kinetic accessibility of the ground state is much lower in the case of a spin glass than in a disordered ferromagnet. This aspect is further analyzed in Fig. 5, where the hamming distance  $d_0^H$  between the current local minimum in a sequence and one of the ground states is mapped against the local minimum energy for 1000 realizations, with 10 monotonic sequences each. The trajectory maps in the  $(d_0^H, E^{LM})$  space very clearly show the funnel-like state space of the DF system. Differently, although the lowest energies reached during the relaxation by the SG systems are very close to the ground states, the systems are far away from reaching the global minimum. The SG system is trapped in low local minima that are close to the ground state energy, although far away in terms of hamming distances. The maps introduced in Fig. 5 clearly illustrate, on one hand, how the DF system is *driven* toward one of the ground states and, on the other hand, how the SG system becomes trapped roughly midway between the two ground states.

In conclusion, we have analyzed structural properties of the state space in both SG and DF systems, which are relevant to the relaxation dynamics. By introducing the DRS as a tool to directly relate topological information to the low-temperature dynamics, the two major features, disorder and frustration, are separately explored: the first is mainly responsible for the barrier structures and their magnitudes, while the latter reduces the funnel-like state space of DFs to a trapping landscape of SGs, reflected in a clear increase in the number of states per valley as well as high hamming distances between the low energy states, which are dynamically relevant and the global minimum. Due to the short-range character of the considered Ising spin systems, good self-averaging properties for the mean energy were found, at least up to a time scale at which half of the energy journey is achieved, allowing infinite volume predictions. The analysis is based only on the topology of the state space and it is in quantitative agreement with low-temperature Monte Carlo Metropolis runs and in qualitative agreement with experiments.

<sup>1</sup>K. D. Ball and R. S. Berry, J. Chem. Phys. **111**, 2060 (1999).

<sup>2</sup>C. Levinthal, J. Chem. Phys. **65**, 44 (1968).

<sup>3</sup>J. L. van Hemmen, Phys. Rev. A **34**, 3435 (1986).

<sup>4</sup>J. P. Garrahan, E. Moro, and D. Sherrington, Quant. Finance **1**, 246 (2001).

<sup>5</sup>D. J. Wales, *Energy Landscapes* (Cambridge University Press, Cambridge, 2003).

<sup>6</sup>C.-Y. Lin, C.-K. Hu, and U. H. E. Hansmann, Phys. Rev. E **64**, 052903 (2001).

<sup>7</sup>P. Garstecki, T. X. Hoang, and M. Cieplak, Phys. Rev. E **60**, 3219 (1999).

<sup>8</sup>M. A. Miller and D. J. Wales, J. Chem. Phys. **111**, 6610 (1999).

<sup>9</sup>D. J. Wales and T. V. Bogdan, J. Phys. Chem. B **110**, 20765 (2006).

<sup>10</sup>E. Vincent, J. Hammann, and M. Ocio, *Recent Progress in Random Magnets* (D. H. Ryan, Singapore, 1998).

<sup>11</sup>P. Sibani and K. H. Hoffmann, Phys. Rev. Lett. **63**, 2853 (1989).

<sup>12</sup>S. Schubert and K. H. Hoffmann, Europhys. Lett. **66**, 118 (2004).

<sup>13</sup>E. Vincent, V. Dupuis, M. Alba, J. Hammann, and J.-P. Bouchaud, Europhys. Lett. **50**, 674 (2000).

<sup>14</sup>A. G. Schins, A. F. M. Arts, and H. W. de Wijn, Phys. Rev. Lett. **70**, 2340 (1993).

<sup>15</sup>H. Mamiya, I. Nakatani, and T. Furubayashi, Phys. Rev. Lett. **82**, 4332 (1999).

<sup>16</sup>S. Franz, M. Mezard, F. Ricci-Tersenghi, M. Weigt, and R. Zecchina, Europhys. Lett. **55**, 465 (2001).

<sup>17</sup>D. J. Wales, Int. Rev. Phys. Chem. **25**, 237 (2006).

<sup>18</sup>W. Krauth and O. Pluchery, J. Phys. A **27**, L715 (1994).

<sup>19</sup>R. S. Berry and R. Breitengraser-Kunz, Phys. Rev. Lett. **74**, 3951 (1995).

<sup>20</sup>C. D. Simone, M. Diehl, M. Jünger, P. Mutzel, G. Reinelt, and G. Rinaldi, J. Stat. Phys. **84**, 1363 (1996).